# Supplementary Information

## Hiding a Realistic Object Using a Broadband Terahertz Invisibility Cloak

Fan Zhou[1]*, Yongjun Bao[1]*, Wei Cao[2]*, Colin Stuart[1], Jianqiang Gu[2], Weili Zhang[2], and Cheng Sun[1†]

[1] Mechanical Engineering Department, Northwestern University, Evanston, IL 60208, USA.
[2] School of Electrical and Computer Engineering, Oklahoma State University, Stillwater, Oklahoma 74078, USA

* These authors contribute equally to this work
† To whom correspondence should be addressed. E-mail: c-sun@northwestern.edu

**Three-dimensional fabrication using projection microstereolithography**

The permittivity variation of the designed cloak pattern is realized by fabricating effective media consisting of high aspect-ratio subwavelength holes inside a polymer host. Although the pixels on the dynamic mask are presented in the discrete form, the grayscale of individual pixels can be adjusted so the hole's size can be tuned with a sub-pixel level of precision. As illustrated in Fig. S1a, in order to fabricate a square hole with width $d$, the grayscale of each individual pixel can be calculated as $grayscale = p \cdot 256$, where $p$ represents the fraction of area occupied by the polymer for each pixel. Herein, grayscale levels of 0 and 255 correspond to minimum and maximum intensity of each pixel, respectively. Before the cloak fabrication, to confirm real fabricated hole exactly match with the designed size, a series of holes with various dimensions were designed and fabricated, and then the difference between the mask value and the fabrication value was compared, as shown in Fig. S1b. It is noted that the fabricated size has a larger error when the hole is small. This is due to the diffusion of radicals into the hole region. The resulting dark polymerization results in the reduction in the hole dimension. Such a non-linear relation in the design and fabricated hole dimension are thus calibrated

experimentally. By incorporating the calibration into the mask design, Fig. S1c illustrates the fabricated hole dimension matches precisely with the designed. The designed grayscale mask of the cloaking and control samples are illustrated in Figs. S1d and S1e, respectively. Inset shows the magnified view of the grayscale mask near the bump.

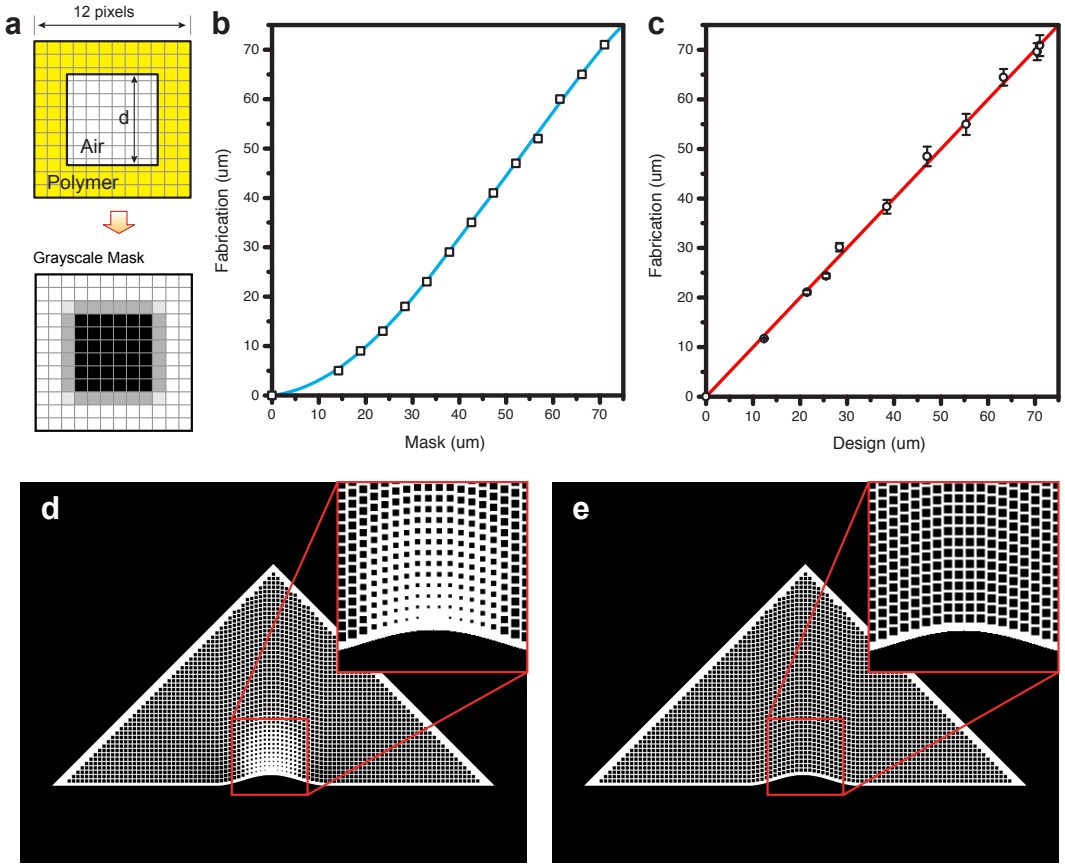


**Fig. S1.** (a) the grayscale of individual pixels can be adjusted so the holes can be fabricated with sub-pixel precision; (b) the mask-fabrication relationship before calibration; (c) the design-fabrication relationship after calibration; (d) designed grayscale mask for fabricating cloaked bump structure; (e) grayscale mask for fabricating the uncloaked bump structure;

After the fabrication, the sample was rinsed in isopropyl alcohol for 48 hours to remove the unpolymerized resin inside the holes. It is confirmed by the crosssectional image of on broken sample shown in Fig. S2a. The high-aspect-ratio holes with well-defined geometry can be clearly observed. Furthermore, a special test sample with exposed

vertical holes are fabricated to exam the geometry along the vertical direction (Fig. S2b). It is clear to see that the hole size changes gradually near the bump and the channel width stays uniform along the vertical direction.

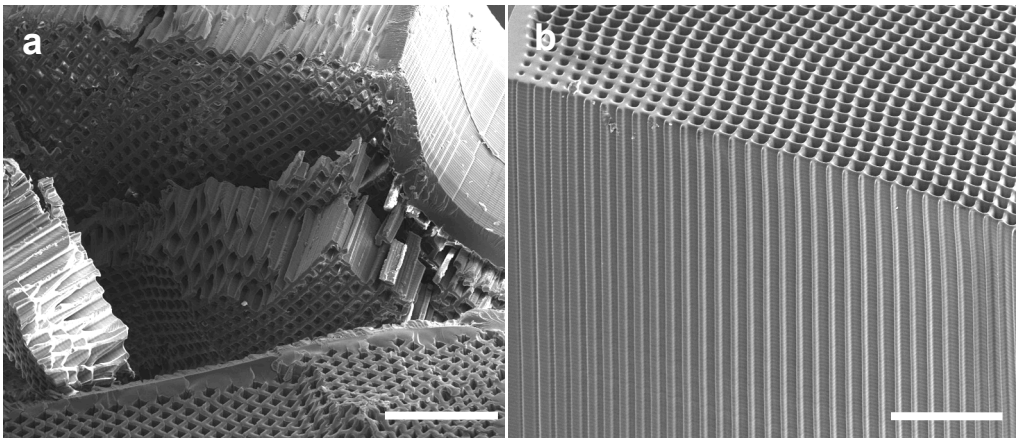


**Fig. S2.** (a) characterization of interior structures of the cloak; (b) cross-section view of the cloak; bar: 500 μ m.

**Angular resolved reflection terahertz time-domain spectroscopy**

Angular resolved reflection terahertz time-domain spectroscopy (THz-TDS, Fig. S3) was employed to assess the performance of the cloaking sample[1,2]. The photoconductive switch-based THz-TDS system was optically gated by 30 fs, 800 nm optical pulses generated from a self-mode-locked Ti:sapphire laser. The THz radiation emitted from a GaAs transmitter was spatially gathered by a hyper-hemispherical silicon lens and then collimated into a parallel beam before entering the cloaking sample at a 45° incident angle. The reflected THz signal through the sample was then detected by a mobile silicon-on-sapphire (SOS) receiver optically excited with fiber-coupled femtosecond pulses[3]. A 1 mm slit was attached to the SOS detector in order to improve the spatial resolution of the measurements. The detector was placed 50 mm away from the output interface of the sample and horizontally scanned to measure the spatial distribution of the THz wave front. Along the horizontal axis, 51 sets of time-domain

signals were measured with a scan step of 0.5 mm. The frequency-dependent THz amplitudes at each spatial position are retrieved by Fourier transform of the measured time-domain signals.

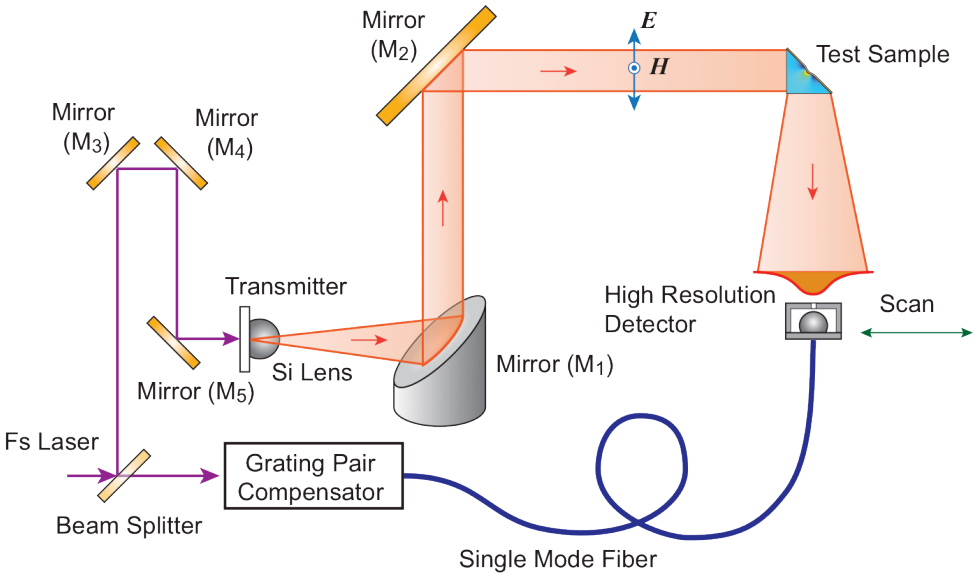


**Fig. S3.** Schematic illustration of angular resolved reflection terahertz time-domain spectroscopy system.

**Terahertz spectroscopy on α-lactose monohydrate**

The THz absorption coefficient of α-lactose monohydrate (Sigma-Aldrich) is measured using a transmission THz-TDS system[4]. 2 mm-thick pure α-lactose monohydrate powder is sandwiched between two 640 μm thick silicon slabs. A silicon-air-silicon stack with 2 mm air gap was used as a reference. $E_{reference}(\omega)$ and $E_{sample}(\omega)$ represent the Fourier-transformed spectra of the transmitted terahertz pulses through the reference and the sample, respectively. The absorption coefficient of the sample powder is extracted based on the transmitted pulses. The complex transmission spectra of the reference $E_{reference}(\omega)$ and the sample $E_{sample}(\omega)$ are given by[2]

$$E_{reference}(\omega) = E_{incident}(\omega) t_{Si-air} t_{air-Si} \exp(ik_0 d)$$

$$E_{sample}(\omega) = E_{in}(\omega) t_{Si-sample} t_{sample-Si} \exp(ikd) \exp(-\alpha d/2)$$

where $E_{incident}(\omega)$ is the incident pulse spectrum, $k_0 = 2\pi/\lambda_0$ and $k = 2\pi n_{sample}/\lambda_0$ are the wave vectors for air and sample, respectively; $n_{sample}$ is the refractive index of the sample, $d$ is the sample thickness, $\lambda_0$ is the free-space wavelength, and $\alpha$ is the absorption coefficient of the sample; $t_{Si\text{-}air}$, $t_{air\text{-}Si}$, $t_{Si\text{-}sample}$, and $t_{sample\text{-}Si}$ are the Fresnel transmission coefficients of the THz pulses propagating through silicon-air, air-silicon, silicon-sample, and sample-silicon interfaces, respectively, which are given by $t_{Si-air} = 2n_{Si}/(1+n_{Si})$, $t_{air-Si} = 2/(1+n_{Si})$, $t_{Si-sample} = 2n_{Si}/(n_{Si}+n_{Sample})$, and $t_{sample-Si} = 2n_{sample}/(n_{sample}+n_{Si})$. The $t_{Si\text{-}sample}$, and $t_{sample\text{-}Si}$ are the complex, frequency-dependent coefficients related to this powder layer sample. The measured absorption coefficient is shown in Fig. S4. Strong absorption peaks at 0.53 THz and 1.37 THz are observed, which is in good agreement with literature[5].

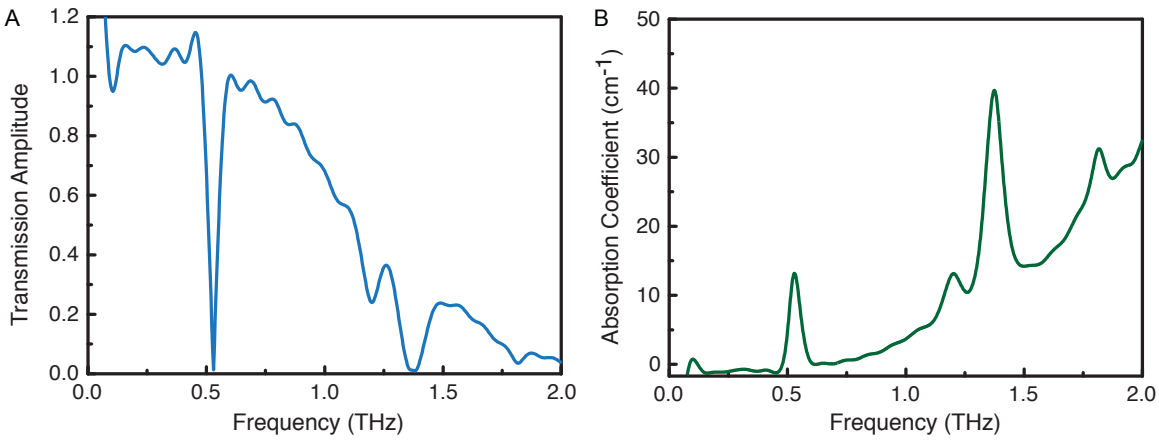


**Fig. S4.** Measured power absorption coefficient of the α-lactose monohydrate powder

**References:**

1 Grischkowsky, D., Keiding, S., Vanexter, M. & Fattinger, C. Far-Infrared Time-Domain Spectroscopy with Terahertz Beams of Dielectrics and Semiconductors. *J Opt Soc Am B* **7**, 2006-2015, (1990).

2 Alu, A. & Engheta, N. Theory and potentials of multi-layered plasmonic covers for multi-frequency cloaking. *New J Phys* **10**, -, (2008).

3 Reiten, M. T., Harmon, S. A. & Cheville, R. A. Terahertz beam propagation measured through three-dimensional amplitude profile determination. *J Opt Soc Am B* **20**, 2215-2225, (2003).

4 Thamizhmani, L., Azad, A. K., Dai, J. M. & Zhang, W. Far-infrared optical and dielectric response of ZnS measured by terahertz time-domain spectroscopy. *Applied Physics Letters* **86**, 131111, (2005).

5 Brown, E. R., Bjarnason, J. E., Fedor, A. M. & Korter, T. M. On the strong and narrow absorption signature in lactose at 0.53 THz. *Applied Physics Letters* **90**, 061908, (2007).